

Ferroelectric-to-relaxor transition behaviour of BaTiO_3 ceramics doped with $\text{La}(\text{Mg}_{1/2}\text{Ti}_{1/2})\text{O}_3$

This article has been downloaded from IOPscience. Please scroll down to see the full text article.

2004 J. Phys.: Condens. Matter 16 2785

(<http://iopscience.iop.org/0953-8984/16/16/003>)

View [the table of contents for this issue](#), or go to the [journal homepage](#) for more

Download details:

IP Address: 129.252.86.83

The article was downloaded on 27/05/2010 at 14:26

Please note that [terms and conditions apply](#).

Ferroelectric-to-relaxor transition behaviour of BaTiO₃ ceramics doped with La(Mg_{1/2}Ti_{1/2})O₃

A N Salak¹, V V Shvartsman, M P Seabra, A L Kholkin and V M Ferreira

Department of Ceramics and Glass Engineering/CICECO, University of Aveiro, 3810-193 Aveiro, Portugal

E-mail: salak@cv.ua.pt

Received 27 December 2003

Published 8 April 2004

Online at stacks.iop.org/JPhysCM/16/2785

DOI: 10.1088/0953-8984/16/16/003

Abstract

Low-frequency dielectric studies were performed on the fine-grain ceramics of BaTiO₃ doped with 2.5 mol% of non-ferroelectric perovskite La(Mg_{1/2}Ti_{1/2})O₃ (BT:2.5% LMT). In addition to the permittivity and P – E hysteresis loop measurements as a function of temperature, local electromechanical properties of BT:2.5% LMT were analysed by piezoresponse force microscopy. It was found that the temperature evolution of the dielectric properties detected by macroscopic methods (average over many grains) is similar to that observed on the nanoscale level (in a single grain). BT:2.5% LMT was revealed to exhibit the typical features of both the ferroelectric and the relaxor. The observed dielectric behaviour is discussed in terms of heterovalent substitution at both A-(Ba²⁺/La³⁺) and B-(Ti⁴⁺/Mg²⁺) perovskite sites.

1. Introduction

Relaxor ferroelectrics with the perovskite structure continue to be attractive objects owing to their prominent dielectric properties. In respect to both scientific and technological points the lead-based compositions, such as Pb(Mg_{1/3}Nb_{2/3})O₃, Pb(Sc_{1/2}Ta_{1/2})O₃, La-substituted Pb(Zr_{1-x}Ti_x)O₃ etc, are mainly explored [1]. Their main drawback is the complicated and health-hazard fabrication because of the high volatility of toxic lead oxide. The search for environment friendly relaxors is recognized therefore to be an important objective. Lead-free perovskite compositions derived from BaTiO₃ (BT) have recently been investigated in respect to their relaxor properties [2–7]. BT-based relaxor materials are mainly produced by the formation of solid solutions with non-ferroelectric perovskites. ‘Virtual’ end members are also explored, i.e. those that do not exist in the perovskite structure due to the high number

¹ Author to whom any correspondence should be addressed.

of vacancies (e.g. $A_{1/2}NbO_3$, $A = Ca, Sr, Ba$ [2]) or packing misfit between A- and B-site cations ($BaBO_3$, $B = Ce, Y$ [3, 4]). A transformation from the classical ferroelectric to relaxor behaviour in the compositions derived from BT is related to the size and charge difference of the ions involved, their polarizability, presence and type of vacancies as well as substitution rates [5–7]. A number of BT-based solid solutions were studied and some features of their evolution in the relaxor state in terms of composition have been revealed [5]. In particular it has been shown that heterovalent cation substitutions at the 6-coordination number crystallographic site are generally responsible for the relaxor behaviour of those systems [2, 6]. Nevertheless, the intermediate state between normal ferroelectric and relaxor has not been thoroughly studied so far in lead-free perovskite systems.

In previous works, the evolution of crystal structure and dielectric properties in the $BaTiO_3$ – $La(Mg_{1/2}Ti_{1/2})O_3$ system have been investigated [8, 9]. $La(Mg_{1/2}Ti_{1/2})O_3$ (LMT) is a low permittivity/low loss microwave dielectric material [9, 10]. It is characterized by a monoclinic perovskite structure ($Z = 4$, space group $P2_1/n$) due to oxygen octahedra tilting and B-site cation (Mg/Ti) ordering [8]. It has been shown that small additions of LMT modify strongly the dielectric response of BT, decreasing the transition temperature to a paraelectric phase about 30 K/1 mol% of LMT [11]. Ceramics of the BT–LMT system were found to exhibit mainly relaxor features at doping levels as low as 5 mol% of LMT.

The present work reports on dielectric properties of the intermediate composition BT:2.5% LMT (ceramics of BT doped with 2.5 mol% of LMT) with respect to the evolution from the normal ferroelectric to relaxor state. The macroscopic dielectric characterization of these ceramics was complemented with the investigation of the local electromechanical properties using piezoresponse force microscopy (PFM).

2. Experimental details

BT:2.5% LMT ceramics were processed from powders obtained by a citrate-based chemical route [10]. This preparation method allows the production of uniform fine-grain ceramics at relatively low sintering temperature. The powders were isostatically pressed into pellets of 10 mm in diameter and about 1 mm thick, and then sintered at 1720 K for 2 h in oxygen gas flow. The relative density of sintered samples was determined by the Archimedes method and their microstructure was examined by scanning electron microscopy (SEM). The samples for all the microscopic investigations were polished and thermally etched 50 K below their sintering temperature for 2 min. Phase analysis and crystal structure determination were performed by x-ray diffraction (XRD) from the powders of the samples ground.

For dielectric measurements the sintered samples were polished to form discs of 0.3–0.5 mm thick, electroded with platinum paste and annealed at 1100 K. Dielectric permittivity (ϵ') was measured as a function of frequency (10^2 – 10^6 Hz) between 10 and 500 K with a heating or cooling rate of 1.5 K min^{-1} . The P – E hysteresis loops were measured in the temperature range of 300–360 K using a standard Sawyer–Tower circuit.

The PFM measurements were performed between 290 and 380 K using a commercial scanning probe microscope (SPM) (Multimode, DI) equipped with a heating stage. The detailed description of the PFM method could be found elsewhere [12]. Briefly the method is based on the detection of local thickness vibration due to the converse piezoelectric effect provoked by an electric field applied between the conducting SPM tip and counter macroscopic electrode. Since the size of the tip is very small (about 10 nm) the field is inhomogeneous and decays very fast into the sample. Thus the response is measured from extremely small regions (of the order of a few tens of nanometres). The domains with opposite polarity are visualized as areas of opposite (bright and dark) contrast. To study the local polarization switching, the

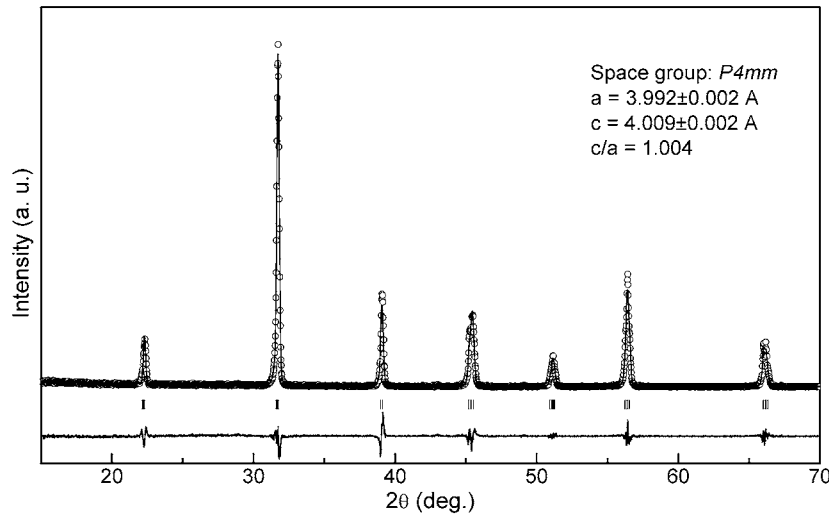


Figure 1. X-ray diffraction data of BT:2.5% LMT (open circles) refined by the Rietveld method (solid curve) and the difference between these (solid curve below the spectrum). The vertical bars correspond to the calculated peak positions.

SPM tip was stopped inside the selected domain and a consecutive sequence of voltage pulses with cyclically varied height from $-V_{\text{dcmax}}$ to $+V_{\text{dcmax}}$ was applied between the tip and the counter electrode. After each pulse the effective local piezoelectric coefficient ($d_{33\text{eff}}$) was measured [13]. The obtained dependence of $d_{33\text{eff}}$ on V_{dc} is an analogue of the piezoelectric hysteresis loop.

3. Results

It was revealed that the obtained ceramics are dense (>95%) and single-phase with a homogeneous grain-size distribution. The XRD pattern of BT:2.5% LMT at room temperature is shown in figure 1. The Rietveld refinement of the spectrum, performed using the FullProf suite [14], has detected a small tetragonal distortion of the perovskite crystal lattice with the ratio $c/a = 1.004$. This value is rather lower than 1.010 for pure BT at the same conditions [15].

Figure 2 displays the dielectric permittivity of BT:2.5% LMT as a function of temperature at different frequencies. One can see that the composition under study undergoes three phase transitions. These are similar to those observed in ferroelectric BT (as temperature increases): from the rhombohedral to orthorhombic phase (at T_1), then to the tetragonal (T_2) and finally to the cubic paraelectric phase (T_C) [16]. However, in the case of BT:2.5% LMT the temperature intervals between transitions are narrower. The transition to the paraelectric phase occurs at about 330 K with a small temperature hysteresis on heating and cooling. The permittivity data were fitted using the modified Curie–Weiss dependence [17]:

$$1/\varepsilon' - 1/\varepsilon'_m = (T - T_m)^\gamma / C', \quad 1 \leq \gamma \leq 2, \quad (1)$$

where ε'_m is the peak value of ε' at the phase transition temperature T_m and C' is a Curie–Weiss-like constant. Note that, for normal ferroelectrics, in particular for BT, T_m is equal to T_C . The exponent γ reflects the character of the phase transition in terms of the dielectric peak broadening. Namely, $\gamma = 1$ indicates the normal ferroelectric one, whereas $\gamma \sim 2$ is related to the so-called ‘complete’ diffuse phase transition [18]. The temperature dependence

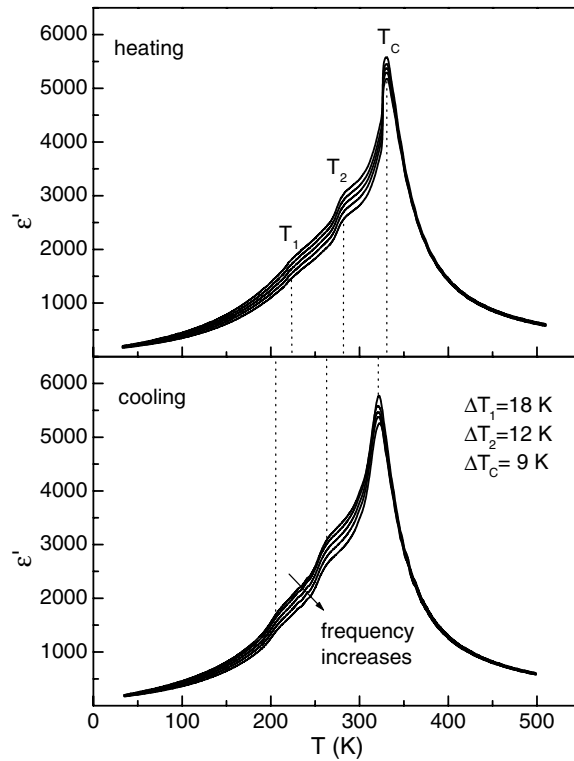


Figure 2. Temperature dependence of the dielectric permittivity (ϵ') at 10^2 , 10^3 , 10^4 , 10^5 and 10^6 Hz on heating and cooling. The values of temperature hysteresis at each phase transition are presented.

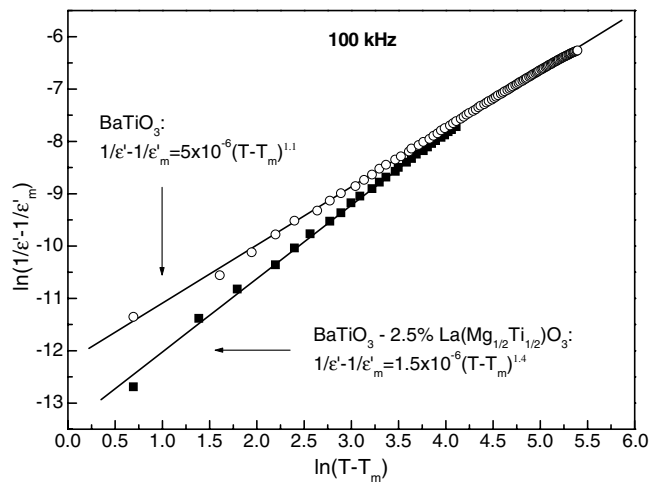


Figure 3. ϵ' versus T fitted by the modified Curie–Weiss relationship—equation (1) (solid curves).

of ϵ' for BT:2.5% LMT follows equation (1) with $\gamma = 1.4$, in contrast to 1.1 for BT ceramics processed under similar conditions (figure 3). For comparison: $\gamma = 1.8$ for the BT:10% LMT composition which exhibits solely relaxor behaviour [11].

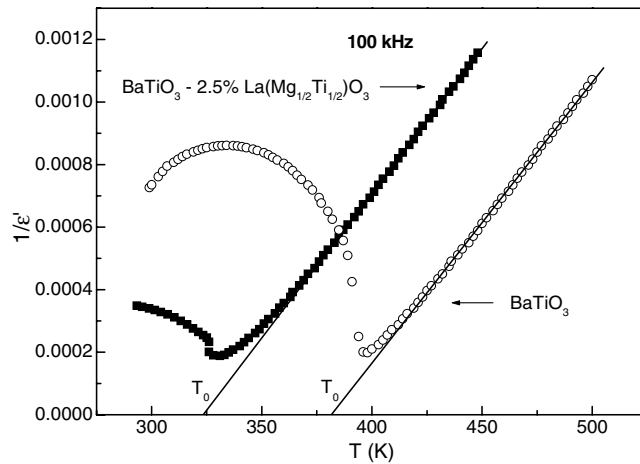


Figure 4. Reciprocal permittivity fitted by the classical Curie–Weiss law (solid lines).

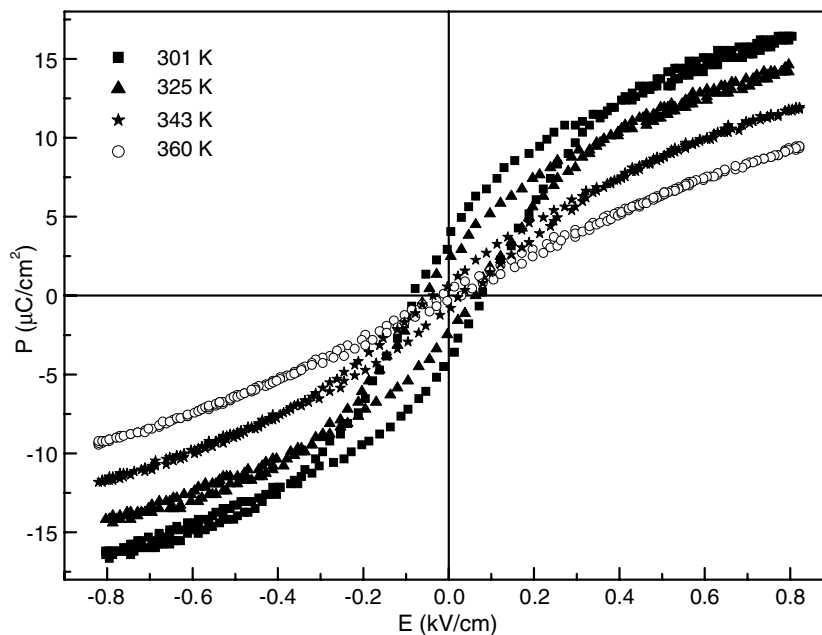


Figure 5. The P – E hysteresis loops of the BT:2.5% LMT sample at various temperatures.

The fit of $\varepsilon'(T)$ with the classical Curie–Weiss law ($\gamma = 1$) indicates that the transition in BT:2.5% LMT is close to a second-order type (figure 4). As seen, the extrapolated Curie–Weiss temperature (T_0) is nearly equal to T_m . Note that for BT $T_0 < T_m = T_C$, which is the signature of a first-order transition. Unlike BT, a deviation from the Curie–Weiss law in BT:2.5% LMT is observed ~ 30 K above the T_m value.

The evolution of the macroscopic hysteresis loops of BT:2.5% LMT with temperature is shown in figure 5. As the temperature increases, the loops degenerate gradually and the so-called slim ones are still observed above T_m . Figure 6 depicts the respective remnant

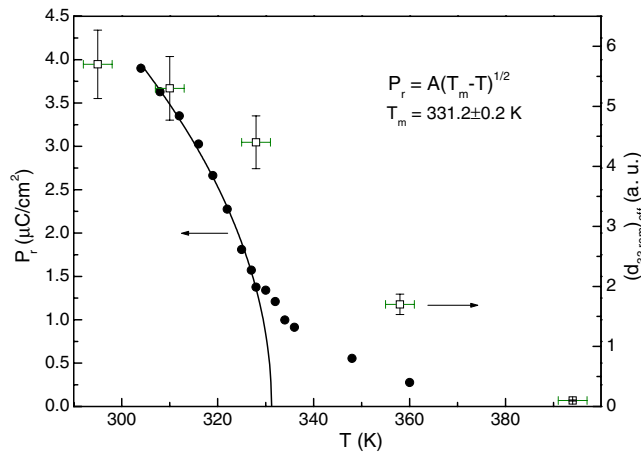


Figure 6. Remnant polarization P_r (solid circles) and remnant $(d_{33})_{\text{eff}}$ coefficient (open squares) as a function of temperature. P_r is fitted by equation (2) (solid curve).

polarization (P_r) as a function of T . The low-temperature part of P_r was found to follow well the relation [19]:

$$P_r = A(T_m - T)^{1/2}, \quad A = \text{constant}. \quad (2)$$

Extrapolation of the remnant polarization with equation (2) gave a zero- P_r value at $T_m = 331$ K, i.e. essentially close to the temperature of the dielectric permittivity peak. At the same time, P_r does not disappear at T_m but demonstrates a slow decay above this temperature.

Figure 7 shows the typical topography and piezoresponse images obtained by PFM at different temperatures. At the room temperature the distinct polydomain structure is observed inside individual grains. In our geometry, the bright and dark areas correspond to domains with the polarization vector pointed correspondingly up and down relative to the figure plane. Grey-contrast areas imply both polarization lying parallel (or almost parallel) to the studied surface or non-piezoelectric phase. The evolution of the piezoresponse images with temperature was found to correlate with the macroscopic observations. Approaching T_m , the piezoresponse signal becomes weaker in accordance with decreasing spontaneous polarization. The domain structure becomes finer; some domains disappear (figures 7(c)–(e)). Finally, above T_m , most of the grains are in the paraelectric state, manifesting the grey contrast. Nevertheless, some small residual domains were observed in the temperature range 10–20 K above T_m [20]. After subsequent cooling back to room temperature the new domain structure, which is different in principle from the initial one, is formed. The local piezoelectric hysteresis loops ($d_{33\text{eff}}$ versus V_{dc}), measured at different temperatures, are shown in figure 8. It was revealed that switchable polarization could be induced by the application of dc voltages even at temperatures above T_m . The temperature dependence of remnant $d_{33\text{eff}}$ measured at $V_{\text{dc}} = 0$ is qualitatively similar to the macroscopic $P_r(T)$ dependence (figure 6).

The additional information on local dielectric properties could be obtained by analysis of the second harmonic of the piezoresponse signal ($I_{2\omega}$). This signal consists of two components. First, the electrostatic contribution is related to the Maxwell force between two opposite electrodes and is proportional to the local dielectric permittivity [13]. Second, the electrostriction contribution is proportional to the square of dielectric permittivity. Thus the variation of the second harmonic signal reflects variation of the local dielectric permittivity. Indeed, the temperature dependence of the second harmonic of the piezoresponse signal shows a maximum near T_m (figure 9).

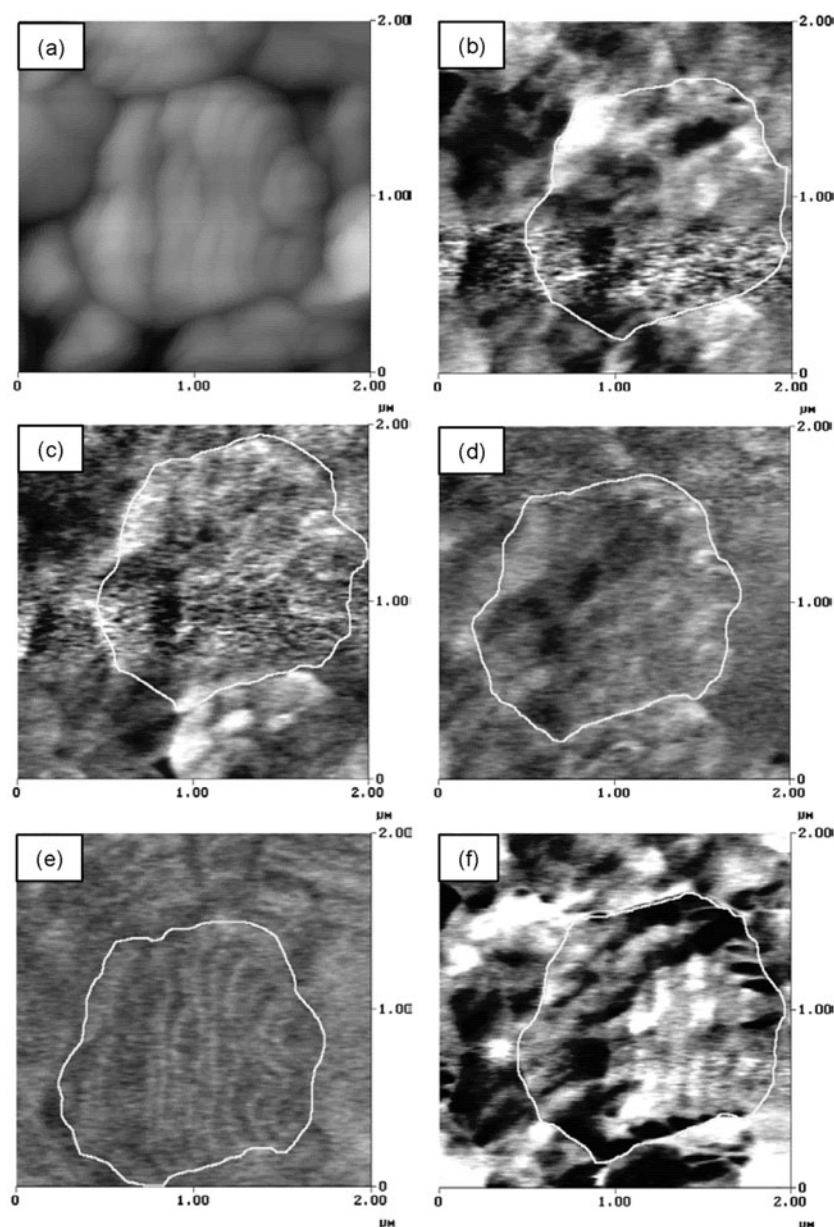


Figure 7. Topography (a) and piezoresponse images ((b)–(f)) of the BT:2.5% LMT ceramics measured at different temperatures: before heating, at 295 K (b), 310 K (c) 330 (d), 395 K (e) and after cooling, at 295 K (f). The white curves indicate the grains boundaries and are drawn to simplify the analysis.

4. Discussion

The results presented above testify that, in general, the BT:2.5% LMT composition exhibits typical ferroelectric features. Its well-characterized sequence of phase transitions, frequency-independent transition into paraelectric phase as well as a tetragonal distortion below the

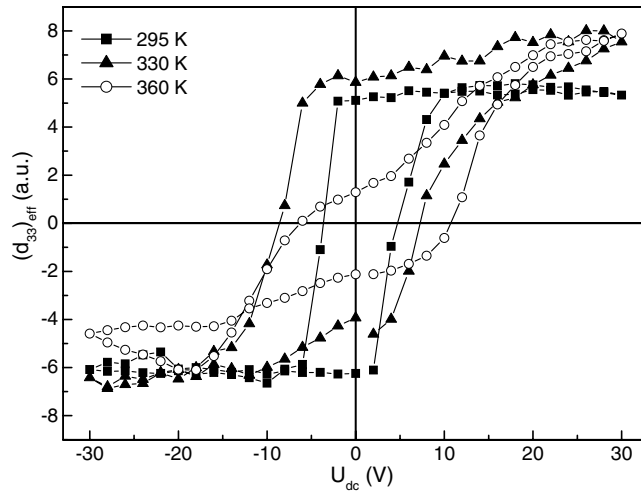


Figure 8. Local piezoresponse hysteresis loops at various temperatures.

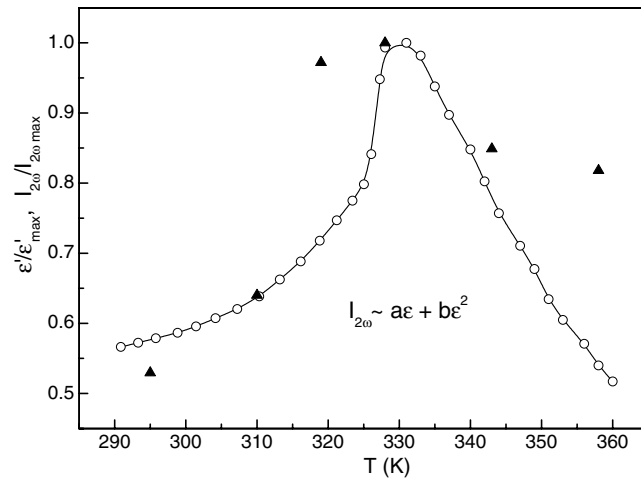


Figure 9. Reduced values of 100 Hz permittivity (open circles) and average intensity of the second harmonic of the piezoresponse signal (solid triangles) plotted as a function of temperature.

transition point T_m are similar to those observed in pure BT. At the same time, the signatures of relaxor behaviour were detected, namely deviation from the classical Curie–Weiss law, change of the order of phase transition at T_m from the first to second one, magnitude of the exponent γ in equation (1) and slim hysteresis loops. Such peculiarities are characteristic of relaxor compositions [21], particularly of those derived from BT [2, 5, 7].

It is important that the temperature evolution of the fundamental dielectric characteristics detected by both macroscopic (average over many grains) and nanoscale (in a single grain) methods was found to be essentially similar. Moreover, no appreciable variance in the dielectric characteristics was detected in different grains examined. One can therefore consider that the observed (ferroelectric-to-relaxor) behaviour of BT:2.5% LMT ceramics is not a result of their macroscopic heterogeneity but rather related to the local chemical structure.

The above-mentioned deviations from the classical ferroelectric behaviour, especially the non-zero value of P_r above T_m , indicate the presence of polar entities in the macroscopically

paraelectric phase of BT:2.5% LMT. As presented in the results section, the remnant $d_{33\text{eff}}$ exhibits a non-zero value even if measured ~ 30 K above T_m . This implies that the applied electric field can induce the local ferroelectric state promoting growth and correlation between these polar entities. It appears to be nanoscale evidence of the presence of polar regions in BT:2.5% LMT above the transition temperature.

The existence of polar nanoregions (PNR) originating from the compositional disorder is generally accepted to be a common characteristic of all the relaxor systems. In lead-containing relaxors such chemical disorder is considered as a source of random fields making the off-centre displacements of Pb²⁺ also random [22]. It is believed that these short-range correlated displacements are the origin of PNR well above T_m . The particular role of the high-polarizable Pb²⁺ cations in lead-based materials has been clearly demonstrated by the evolution of dielectric behaviour in Ba-substituted Pb(Mg_{1/3}Nb_{2/3})O₃ [23]. In the case of lead-free relaxors the situation seems to be rather different. All those were mainly derived from ferroelectric titanates (such as BaTiO₃ [5] and (Na_{1/2}Bi_{1/2})TiO₃ [24]) or niobates (e.g. NaNbO₃ [25]). Unlike Pb-based compositions, the polarization of a B-site cation within the oxygen octahedra is known to be responsible for their ferroelectric properties. Therefore, it seems to be not unexpected that lead-free and lead-based relaxors are also different from a nanostructural point of view [26].

Doping BT with LMT was found to result in strong suppression of the ferroelectric coupling in the former [11]. Let us consider the effect of the LMT doping in terms of the modification of the polar units—TiO₆ octahedra and their surroundings. First, the substitution with smaller La³⁺ offers less space for the Ti⁴⁺ displacements and thereby reduces the macroscopic polarization. It results ultimately in some decrease of T_m . However, this steric effect is apparently dominant only for isovalent substitution at the A-site [5]. Heterovalent doping was found to act in a stronger manner. Regarding La-doped BT ceramics, a decrease of the transition temperature with the doping cation content ($\Delta T_m/\Delta x$) was estimated in both Ba_{1-x}La_{2x/3}TiO₃ (cation vacancies at the A-site) [27] and Ba_{1-x}La_xTi_{1-x/4}O₃ system (cation vacancies at the B-site) [28] to be ~ 19 and 23 K/1 mol% of La, respectively. It should be pointed out that, in the case of the B-site vacancies, the $\Delta T_m/\Delta x$ value is higher and relaxor behaviour appears at smaller value of x . We stress again that indeed the B-site chemical disorder is generally responsible for relaxor properties of BT-based compositions. In the case of BT doped with LMT both A-(Ba²⁺/La³⁺) and B-(Ti⁴⁺/Mg²⁺) substitutions are heterovalent. Strong local deformations and stresses caused by charge and size misfits make displacements of the Ti⁴⁺ cations uncorrelated resulting in the relaxor behaviour. This effect is likely to be stronger when these differences in charge and size are bigger.

In BT:2.5% LMT the content of substituting atoms is apparently too low to break down the ferroelectric coupling that exists in the BT-matrix. Indeed, the cube of $10 \times 10 \times 10$ unit cells contains only 25 La³⁺ and about 12 Mg²⁺ cations on average. Provided that no vacancies appear when BT is doped with LMT, one can suppose that these substituting cations (lanthanum and magnesium) should be close to each other. It means that the concentration of these ‘impurity units’ is too small to allow interaction between them. Therefore these would exist like non-interacting ‘islands’ in the ferroelectric surroundings. This seems to be the reason why BT:2.5% LMT exhibits mainly ferroelectric behaviour.

5. Conclusions

Ceramics of BaTiO₃ doped with 2.5 mol% of La(Mg_{1/2}Ti_{1/2})O₃ (BT:2.5% LMT) exhibit a transition behaviour from ferroelectric to relaxor. Dielectric and structural characterization of this mixed perovskite ceramics has revealed the typical features of normal ferroelectrics, namely the distinctive sequence of phase transitions like those in pure BT, the frequency-

independent transition into paraelectric phase close to second order type as well as the tetragonal distortion below the transition point T_m . At the same time, the signatures of relaxor behaviour were observed, such as deviation from the classical Curie–Weiss law and non-zero remnant polarization above T_m . Temperature evolution of the domain structure detected by piezoresponse force microscopy also testifies the intermediate (between ferroelectric and relaxor) nature of BT:2.5% LMT.

The strong T_m reducing effect observed in BT:2.5% LMT is believed to result from simultaneous heterovalent substitutions at A-(Ba²⁺/La³⁺) and B-(Ti⁴⁺/Mg²⁺) perovskite sites. Due to both size and charge differences, the impurity cations induce local deformations and stresses making uncorrelated the polarization of the Ti⁴⁺ inside the oxygen octahedra. At the same time, in the studied composition the content of substituting atoms is too low to break down the ferroelectric coupling that exists in the BT-matrix.

Acknowledgments

The authors thank Dr D Khalyavin for help with the Rietveld refinement of the XRD data. The authors also acknowledge the Foundation for Science and Technology (FCT-Portugal) for their support (Projects POCTI/40187/CTM/2001 and SFRH/BPD/9214/2002).

References

- [1] Cross L E 1994 *Ferroelectrics* **151** 305
- [2] Ravez J and Simon A 2000 *Phys. Status Solidi* **178** 793
- [3] Chen A, Zhi J and Zhi Y 2002 *J. Phys.: Condens. Matter* **14** 8901
- [4] Zhi J, Chen A, Zhi Y, Vilarinho M P and Baptista J L 1998 *J. Appl. Phys.* **84** 983
- [5] Ravez J and Simon A 1998 *J. Korean Phys. Soc.* **32** S955
- [6] Zhi J, Zhi Y and Chen A 2002 *J. Mater. Res.* **17** 2787
- [7] Komine S and Iguch E 2002 *J. Phys.: Condens. Matter* **14** 2043
- [8] Avdeev M, Seabra M P and Ferreira V M 2002 *J. Mater. Res.* **17** 1112
- [9] Seabra M P, Salak A N, Ferreira V M, Vieira L G and Ribeiro J L 2003 *Ferroelectrics* **294** 165
- [10] Seabra M P and Ferreira V M 2002 *Mater. Res. Bull.* **37** 255
- [11] Salak A N, Seabra M P and Ferreira V M 2004 *J. Am. Ceram. Soc.* **87** 216
- [12] Abplanalp M, Eng L M and Gunter P 1998 *Appl. Phys. A* **66** S231
- [13] Zavala G, Fendler J H and Troiler-McKinstry S 1997 *J. Appl. Phys.* **81** 7480
- [14] Rodriguez-Carvajal J 1993 *Physica B* **192** 55
- [15] Harada J, Pedersen T and Barnea Z 1970 *Acta Crystallogr. A* **26** 336
- [16] Lines M E and Glass A M 1977 *Principles and Applications of Ferroelectric and Related Materials* (London: Oxford University Press)
- [17] Uchino K and Nomura S 1982 *Ferroelectrics* **44** 55
- [18] Kirillov V V and Isupov V A 1973 *Ferroelectrics* **5** 3
- [19] Kittel C 1996 *Introduction to Solid State Physics* (New York: Wiley)
- [20] Salak A N, Shvartsman V V, Seabra M P, Kholkin A L and Ferreira V M 2004 *Ferroelectrics* at press
- [21] Cross L E 1987 *Ferroelectrics* **76** 241
- [22] Egami T 2002 *Ferroelectrics* **267** 101
- [23] Butcher C J and Thomas N W 1991 *J. Phys. Chem. Solids* **32** 595
- [24] Säid S and Mercurio J P 2001 *J. Eur. Ceram. Soc.* **21** 1333
- [25] Raevski I P and Prosandeev S A 2002 *J. Phys. Chem. Solids* **63** 1939
- [26] Kreisel J, Bouvier P, Dkhil B, Thomas P A, Glazer A M, Welberry T R, Chaabane B and Mezouar M 2003 *Phys. Rev. B* **68** 14113
- [27] Ravez J and Simon A 2000 *Solid State Sci.* **2** 525
- [28] Morrison F D, Sinclair D C and West A R 1999 *J. Appl. Phys.* **86** 6355